Macromolecular Research, Vol. 17, No. 10, pp 763-769 (2009)

Osmotic Cross Second Virial Coefficient (B_{23}) of Unfavorable Proteins : Modified Lennard-Jones Potential

Sang Ha Choi and Young Chan Bae*

Division of Chemical Engineering and Molecular Thermodynamics Lab., Hanyang University, Seoul 133-791, Korea

Received January 12, 2009; Revised April 8, 2009; Accepted April 11, 2009

Abstract: A chromatographic method is used to measure interactions between dissimilar proteins in aqueous electrolyte solutions as a function of ionic strength, salt type, and pH. One protein is immobilized on the surface of the stationary phase, and the other is dissolved in electrolyte solution conditions flowing over that surface. The relative retention of proteins reflects the mean interactions between immobile and mobile proteins. The osmotic cross second virial coefficient calculated by assuming a proposed potential function shows that the interactions of unfavorable proteins depend on solution conditions, and the proposed model shows good agreement with the experimental data of the given systems.

Keywords: chromatography, pair potential function, osmotic cross second virial coefficient, MLJ potential.

Introduction

Proteins are currently of great interest in nowadays due to their wide suitability for various applications in fields of biotechnology and the pharmaceutical industry. The exact survey of the thermodynamic properties of protein solutions, therefore, plays an important role in biochemical technology. The osmotic second virial coefficient is one property that shows the nonidealities of protein solutions. Numerous studies have been reported on the experimental osmotic second virial coefficient of the protein(2)/protein(3) systems.

Moon *et al.*[1] measured a series of osmotic pressure data of aqueous solutions containing hen-egg-white lysozyme and any one of the following salts: $(NH_4)_2SO_4$, $(NH_4)_2C_2O_4$, and $(NH_4)_2HPO_4$ at ionic strength 1, 3, or 3.5 M, respectively. They used the McMillan–Mayer osmotic virial equation[2] and Derjaguin-Landau-Verwey-Overbeek (DLVO) theory[3] to correlate their experimental data. The regressed osmotic second virial coefficients and the Hamaker constants of lysozyme were different in various electrolyte solutions at different ionic strengths and pH values.

Haynes *et al.*[4] determined the osmotic pressure at 25 °C for aqueous α-chymotrypsin solutions containing potassium sulfate or a sodium phosphate buffer. Osmotic pressures versus α-chymotrypsin concentrations (1-10 g/L) were reported at various pH values for the 0.1 M potassium sulfate solutions and the 0.1 M sodium phosphate solutions. For the sulfate system at pH 3, osmotic pressures versus α-chymotrypsin concentrations were measured at three different ionic strengths (0.03, 0.15, and 0.3 M). These data covered the protein concentration range from 1 to 40 g/L. They correlated their osmotic pressure data with the osmotic virial equation. The osmotic second virial coefficient (B_{22}) and number-average molecular weight (M_2) of α-chymotrypsin were obtained from the plot of π/c_2 versus c_2. They found that the values of B_{22} and M_2 varied with different ionic strengths and pH values. The regressed molar mass of α-chymotrypsin are from 27.4 to 37.7 kg/mol. They used the relation between virial coefficients and potentials of mean force to determine the interactions of charged protein molecules. Some more complete potential functions including charge-charge repulsion, charge-dipole, dipole-dipole, dipole-induced dipole, and charge-induced dipole attraction terms, which were previously reported by Vilker *et al.*[5] and Phillies,[6] were then adopted by Haynes *et al.*. They also indicated that the effect of ion binding and the three-body interactions should be considered at high protein concentrations in order to improve their correlation. Weak protein interactions are characterized in terms of the osmotic second virial coefficient, which has been shown to correlate with protein phase behavior. Curtis *et al.*[7] determined the osmotic second virial coefficient of lysozyme (1-5 g/L) in saline solutions with low-angle laser-light scattering and discussed various contributions to the virial coefficient. Tessier *et al.*[8] measured protein interactions using self-interaction chromatography, in which protein is immobilized on chromatographic particles and the retention of the same proteins is measured in isocratic elution.

Almost all experimental studies in the literature have focused on single protein system.[9-12,23] However, we require

*Corresponding Author. E-mail: ycbae@hanyang.ac.kr

extension to systems where two or more different proteins are present in solution. Multi-protein systems require not only information for protein(2)-protein(2) self interaction, but also for cross protein(2)-protein(3) interactions. Measurements of the osmotic cross second virial coefficient B_{23} for protein(2)-protein(3) pair provide useful data for determining optimum conditions to precipitate or crystallize a target protein from an aqueous protein mixture. We have described the use of chromatography to measure protein-protein interactions in two-protein systems. To measure protein(2)-protein(3) interactions, one protein is immobilized on a porous stationary phase while the other protein passes through the column in the mobile phase. The average retention time of the mobile-phase protein provides a quantitative measure of the mobile-protein/immobile-protein interaction. Also, we must account for interactions between unfavorable proteins that are not present when measuring favorable protein interactions. In describing the attractive forces between two adjacent molecules, the square-well (SW) fluid model has been extensively studied because it is useful as the first approximation to the understanding of properties of real fluids with spherically shaped molecules. In fact, properties of real fluids can be approximated by those of an SW fluid (SWF) with suitably chosen potential depth and range. Moreover, the thermodynamic properties of an SWF are easier to determine theoretically than those of other fluids having more complicated potentials. This, in particular, is the case for perturbation theories,[13,14] from which the thermodynamic properties of SWFs can be obtained analytically.[15]

However, the SW model appears to be a rather crude approximation of a real fluid. To obtain the thermodynamic properties of a real fluid from those of a fluid with a model potential, it seems advisable to use a potential model that more closely mimics the shape of the real intermolecular potential. Unfortunately, in most cases this can lead to non-analytical expressions for the theoretically obtained thermodynamic properties, which reduce their usefulness. In this study, we develop a new analytical potential function for predicting properties of protein solutions by introducing the modified Lennard-Jones (MLJ) potential to explain the short-range interaction between protein molecules. The MLJ potential function is as simple as the SW potential but more flexible and realistic compared with most existing potential functions. In addition, we demonstrate that the new potential function is capable of predicting the osmotic cross second virial coefficient of the real protein solutions with great accuracy.

Experimental

Materials and Equipment. Lysozyme from chicken egg white, bovine serum albumim (BSA) from pH 7, suitable for diluent in ELISA applications, min. 98% (electrophoresis), lyophilized powder, reagent-grade NaCl, NH_4Cl, Na_2SO_4, tris(hydroxymethly aminomethane), sodium phosphate buffer, and sodium cyanoborohydride were from Sigma and Aldrich. Periodate-activated agarose (P-9967) from Sigma was used as the stationary phase for all chromatographic measurements. Stationary phases were packed into a 10 cm × 0.5 cm inner diameter chromatographic column in Amersham Pharmacia ÄKTA FPLC system.

Experimental Procedures. All solutions were prepared with deionized water and buffers were prepared by adding necessary amounts of sodium phosphate. To conduct our experiments, we have routine chromatography methods reported by Teske *et al.*,[16] and Domen *et al.*[17] for stationary phase of lysozyme to periodate-activated agarose. 4 mL of periodate-activated agarose were mixed with 4 mL of protein-containing coupling buffer. Protein concentrations were 20 mg. The coupling buffer used for the preparation of the lysozyme-loaded stationary phase for BSA-lysozyme experiments was 100 mM sodium phosphate at pH 7.0 and then 30 mg of sodium cyanoborohydride were added to the agarose-buffer mixture. In FPLC system, a pulse of dilute aqueous acetone (2% v/v) was injected to determine the extent of dispersion or channeling in the packed bed. If the exiting acetone peak was not symmetric, the column was repacked. Experiments were conducted at a flow rate of 0.2 mL/min. Protein concentration is 0.5 mg/mL, and 0.1 mol ionic strength were added to 20 mM tris(hydroxymethly aminomethane) buffer solution. Protein solutions were injected at each of solution conditions.

Chromatographic Determination of B_{23}. Teske's analysis of results from quantitative affinity chromatography for single-protein systems demonstrated the importance of considering the interaction of the mobile-phase protein with clusters of immobilized proteins on the stationary-phase surface. The osmotic second virial coefficient for the protein(2)-protein(2) interaction as:

$$B_{22} = \frac{-K}{N} = \frac{\overline{V_0} - \overline{V_r}}{m_{ad}N} \tag{1}$$

where K is the distribution factor and N is the number of accessible immobilized protein molecules per mass of adsorbent, m_{ad}, and the retention volumes of the mobile protein on the protein-loaded and protein-free stationary phases are $\overline{V_r}$ and $\overline{V_0}$ respectively. To calculate the osmotic cross second virial coefficient, B_{23}, a model for the potential of mean force, $\omega_{23}(r)$, for the protein(2)-protein(3) interaction is shown by McMillan and Mayer. The osmotic cross second virial coefficient, B_{23} is related to $\omega_{23}(r)$ by:

$$B_{23} = -2\pi\int_0^\infty \left[\exp\left(\frac{-\omega_{23}(r)}{kT}\right) - 1\right] r^2 dr \tag{2}$$

where k is Boltzmann's constant.

Table I. Energy Parameter ε/k as a Function of Ionic Strength for Each of Salts at 25 °C

	Numerical Formulas for ε
	pH=7.0
NaCl	ε/k = 75.41463 + 5.068158Ln(I)
NH_4Cl	ε/k = 75.17570 + 4.613923*Ln(I)
Na_2SO_4	ε/k = 75.349 + 4.40776*Ln(I)

Model Descriptions.

The Pair-Potential Function: With the development of statistical thermodynamics on the theories of fluids, many EOSs have been developed in terms of parameters characterizing the intermolecular forces. Recent examples[24] are almost based on many different types of potentials such as the Hard-Sphere (HS) potential, the Lennard-Jones (LJ) potential, the SW potential, the inverse power potential, and the hard-core Lennard-Jones (HCLJ) potential. These potential eqs. (3) to (7) are listed in Table II. In this study, we modified the LJ potential to broaden its applicability to many different types of fluids.

MLJ Potential: It is desirable that a potential function be able to represent intermolecular forces for various kinds of fluid; however, it must still be simple in mathematical form. It is difficult to satisfy these requirements simultaneously.[19] In this work, we propose a MLJ potential function that can cover various interaction ranges, which is adjusted by a temperature-dependent parameter. It can be expressed as follows:

$$\omega(r) = \begin{cases} \infty & (0<r<\sigma) \\ -\varepsilon & (\sigma<r<2\sigma/A(\tilde{T})) \\ \dfrac{\varepsilon}{1-A(\tilde{T})\left(\dfrac{r}{\sigma}\right)} & (2\sigma/A(\tilde{T})<r<\lambda\sigma) \\ 0 & (r>\lambda\sigma) \end{cases} \tag{8}$$

where r is the center-to-center distance between two adjacent molecules, σ is the collision diameter, ε is the minimum potential energy, $\tilde{T} = kT/\varepsilon$ is the reduced temperature with Boltzman constant k, and $A(\tilde{T})$ is the temperature-dependent parameter that is determined from the computer simulation data for the compressibility factor. Eq. (9) is obviously more realistic and flexible than those of previously mentioned as the value of $A(\tilde{T})$ is adjusted with diverse conditions in addition to the parameters, σ and ε. We assume that $A(\tilde{T})$ is dependent on temperature and obtained from the computer simulation data for the compressibility factor at various temperatures.[20] In Figure 1, calculated values of $A(\tilde{T})$ are plotted against the reduced temperature and the adjusted temperature range is 273 to 450 Kelvin. To simply correlate with simulation data, $A(\tilde{T})$ is suggested:

$$A(\tilde{T}) = \frac{1.761 - 1.579\tilde{T}}{1-\tilde{T}} \tag{9}$$

When compared with calculated values of $A(\tilde{T})$, eq. (9) reproduces those values fairly well.

Table II. The Potential Equations

	Potential Equation		
HS potential	$\omega(r) = \begin{cases} \infty & (0<r<\sigma) \\ 0 & (r>\sigma) \end{cases}$	(3)	σ: Hard sphere diameter
LJ potential	$\omega(r) = 4\varepsilon\left[\left(\dfrac{\sigma}{r}\right)^{12} - \left(\dfrac{\sigma}{r}\right)^{6}\right]$	(4)	σ: Collision diameter ε: Depth of the energy well
SW potential[18]	$\omega(r) = \begin{cases} \infty & (0<r<\sigma) \\ -\varepsilon & (\sigma<r<R\sigma) \\ 0 & (r>R\sigma) \end{cases}$	(5)	σ: Collision diameter ε: Depth of the energy well
Inverse-power potential	$\omega(r) = \begin{cases} \infty & (0<r<\sigma) \\ -\varepsilon\left(\dfrac{\sigma}{r}\right)^{n} & (r>\sigma) \end{cases}$	(6)	r : Center-to-center distance
HCLJ potential	$\omega(r) = \begin{cases} \infty & (0<r<\sigma) \\ -\varepsilon & (\sigma<r<2^{1/6}\sigma) \\ 4\varepsilon[(\sigma/r)^{12} - (\sigma/r)^{6}] & (r>2^{1/6}\sigma) \end{cases}$	(7)	σ: Collision diameter ε: Depth of the energy well

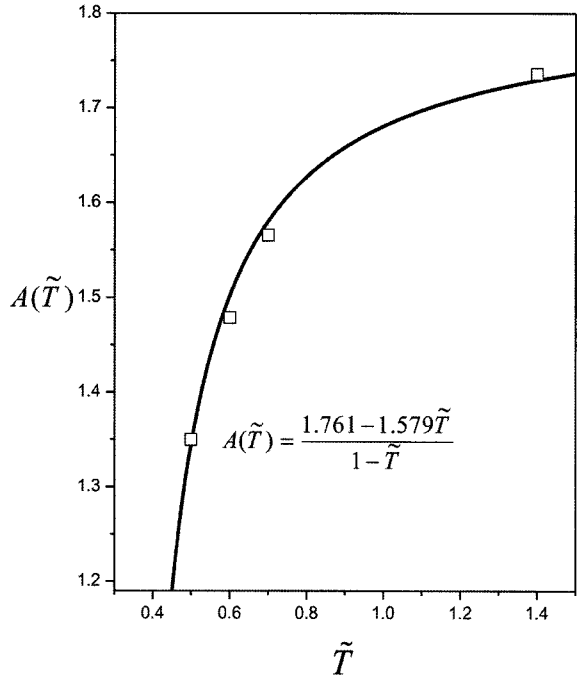

Figure 1. The calculated values of $A(\tilde{T})$ plotted against $\tilde{T}$.

Results and Discussion

Compressibility Factor. In this section, we calculated the compressibility factor of the SWF at $\tilde{T}$=1.75, 2.5, and 3.0, combined with eq. (9). The value of λ is taken as 3.0 because this value has been used for the SWF by numerous researchers to simulate the properties of this fluid. Simultaneously, our model, MLJ potential function, is also compared with several potential functions that come from different types of pair-potential functions: the HS potential, the LJ potential, the SW potential, the inverse-power potential, and the HCLJ potential. The results are given together with the simulation data in Figure 2. Dark squares indicate computer simulation data from Nicolas *et al.*[21] and lines are calculated by denoted in the figure. The proposed MLJ model gives an excellent agreement with the simulation data in the entire density region among other potential functions.

BSA-Lysozyme Interactions. Figure 3 shows the experimental retention volume data for all systems studied using chromatography. It should be noted that the chromatography data are plotted as a function of concentration of salts, without considering the buffer concentration, and the pH at which the chromatography data were fixed at 7.0. At low ionic strength, our results show that mobile phase protein comes out later than the high salt concentration at an exit of the column. The reason that the retention volume increases at low ionic strength may be due to an increase in attractive interactions. At high ionic strength, it may be increased in repulsive interaction due to the binding of the salt ions. The effects produce the same results at the osmotic cross second virial coefficient.

Estimation of Cross Interaction Energy Parameter, ε. In general, protein interactions are known to be governed by many factors, such as pH, surface hydrophobicity, surface-charge distribution, salt-type, and salt concentration.[5] In this study, the cross energy parameter, ε, for NaCl, NH_4Cl, Na_2SO_4 is obtained from the experimental data using the MLJ potential function at pH 7.0. The calculated ε for corresponding conditions are shown in Figures 4-6. For simplicity, those are assumed to have parabolic shapes, and be quadratic functions of ionic strength.

Osmotic Cross Second Virial Coefficient, B_{23}, for BSA-Lysozyme. In Figures 7-9, the osmotic cross second virial coefficient, B_{23}, of BSA-lysozyme in NaCl, NH_4Cl, Na_2SO_4

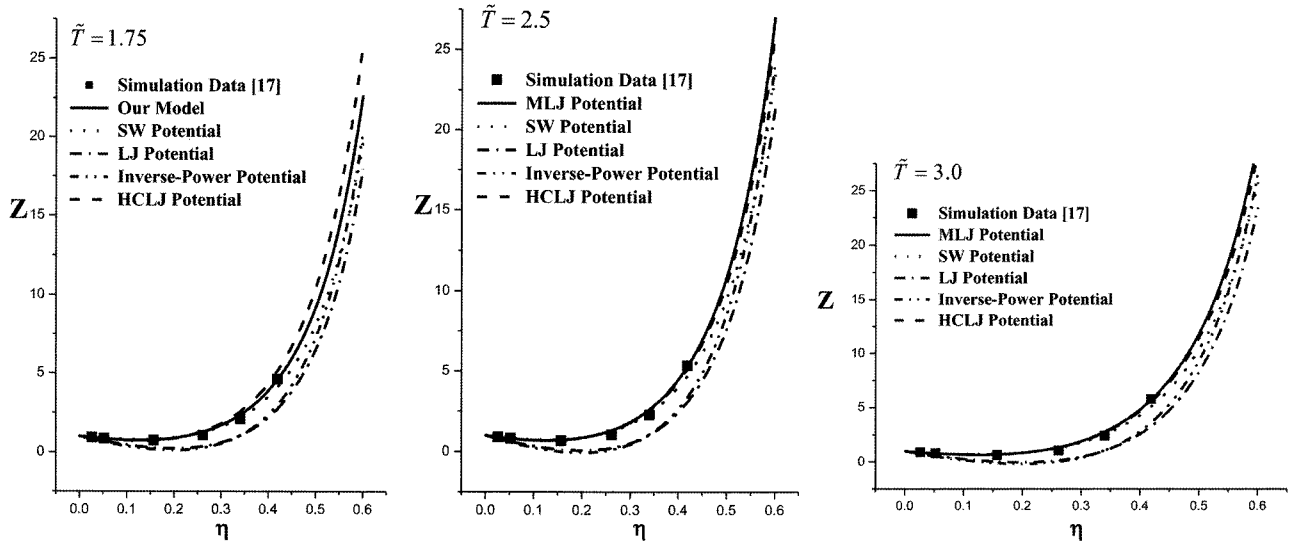

Figure 2. Predictions of the compressibility factor for the SWF at $\tilde{T}$=1.75, 2.5, and 3.0. Dark squares are computer simulation data reported by Largo and Solana.[20] Solid and dotted lines are calculated by the MLJ and SW-fluid model, respectively.

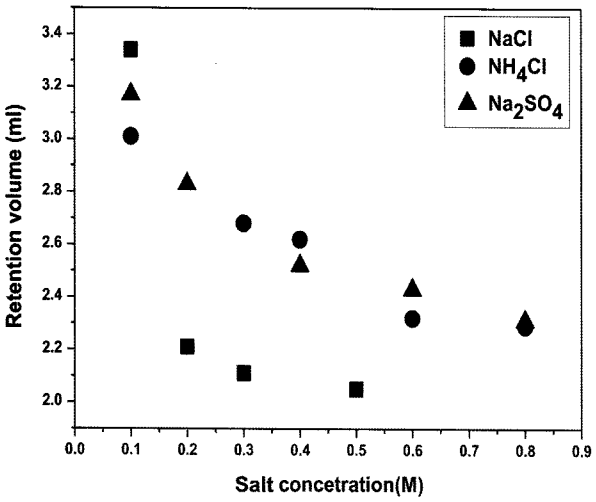

Figure 3. The experimental retention volume plotted against several salts concentration at pH 7.0 with using chromatography method. Dark squares are sodium chloride, circles are ammonium chloride, and triangles are sodium sulfate.

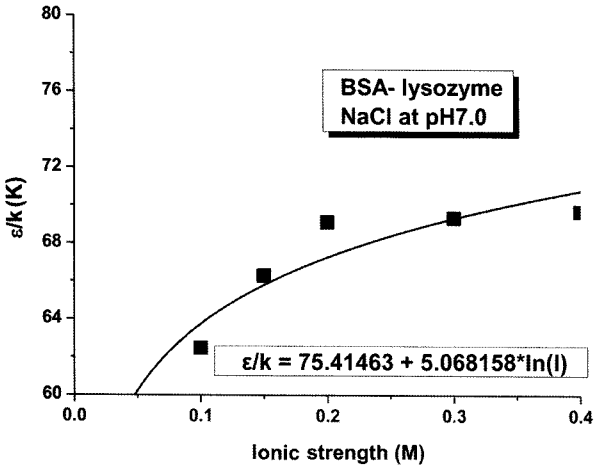

Figure 4. The cross interaction energy as a function of ionic strength for BSA-lysozyme. The calculated values of plotted against 0.1 M NaCl at pH 7.0. Dark squares are calculated by using eq. (1) and (2) with experimental data. Solid line is calculated by correlating equation given.

solutions are plotted against ionic strength for pH 7.0. For experimentally observed B_{23} of BSA-lysozyme interactions, dark circles indicate experimental data and squares are calculated values based on the MLJ model. In eq.(2), the model parameters required to calculate B_{23} are already determined from the computer simulation data for the compressibility factor or experimental data of protein solutions in previous sections, and no additional adjustable parameters are needed to predict the osmotic pressure.

At pH 7.0, BSA-lysozyme interactions are strongly attractive at low ionic strength, but become less attractive with increased ionic strength. The effect of different salts on the

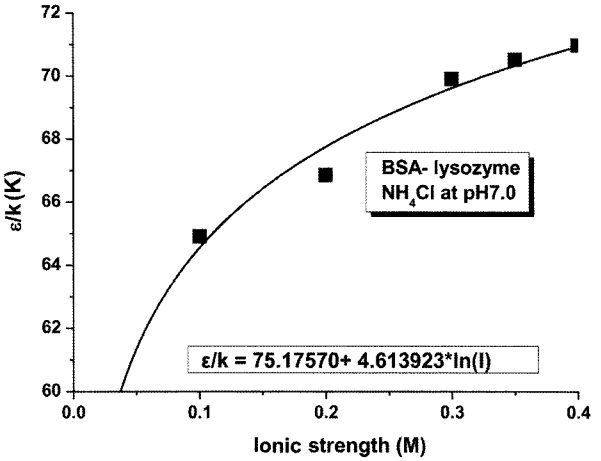

Figure 5. The cross interaction energy as a function of ionic strength for BSA-lysozyme.

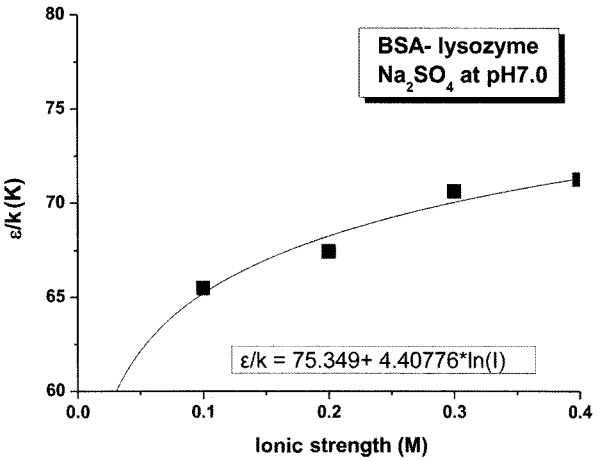

Figure 6. The cross interaction energy as a function of ionic strength for BSA-lysozyme.

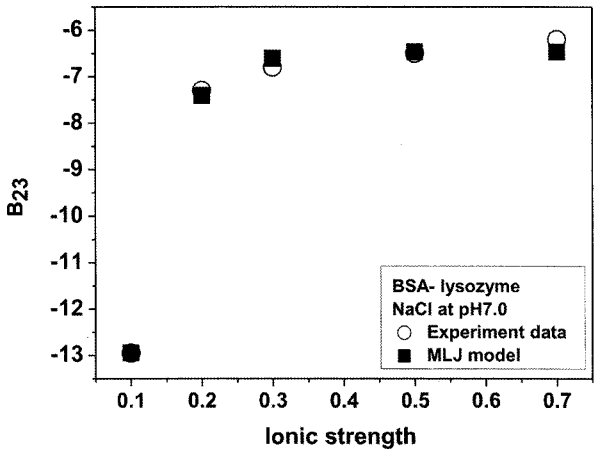

Figure 7. The cross 2nd virial coefficient at 25 °C at pH7.0 as a function of sodium chloride concentration for BSA-lysozyme interactions. Circle symbols are experimental data and squares are calculated by eq. (2) with the MLJ potential function.

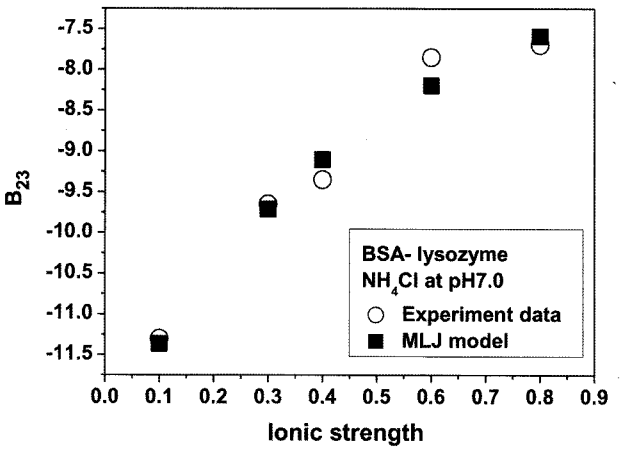

Figure 8. The cross 2nd virial coefficient at 25 °C at pH 7.0 as a function of ammonium chloride concentration for BSA-lysozyme interactions.

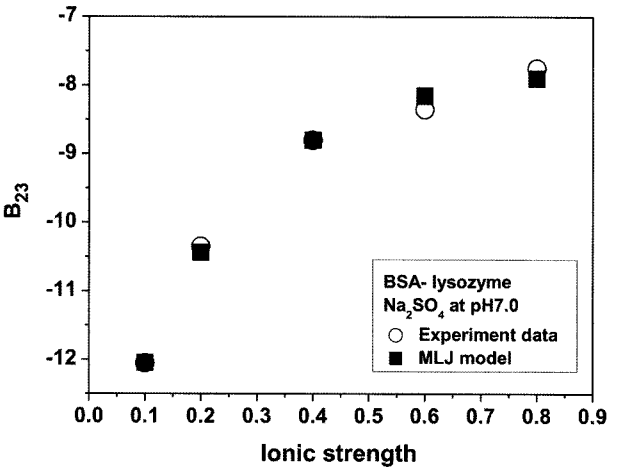

Figure 9. The cross 2nd virial coefficient at 25 °C at pH 7.0 as a function of sodium sulfate concentration for BSA-lysozyme interactions.

interaction is more difficult to explain. The salts with divalent ions tend to screen the interaction more than those with only monovalent ions. In each of the salts, the predictions from theoretical models show agreements from experimental data at entire ionic strengths. At pH 7.0, two proteins are oppositely charged and the electrostatic potential is attractive.[22] The magnitude of the electrostatic potential is a strong function of ionic strength. As the ionic strength rises, the charges on the protein molecules are screened and the strength of electrostatic interaction declines. However, with the potential-of-mean force model given, this effect cannot be solely attributed to electrostatic interactions because the cross interaction energy parameter is a function of ionic strength. Figure 10 shows the effect of NaCl salts on BSA-lysozyme interactions as a function of pH at fixed ionic strength of 0.1 mol. At low pH, the interaction is weak, usually mildly attractive.[16] As pH rises, BSA-lysozyme interac-

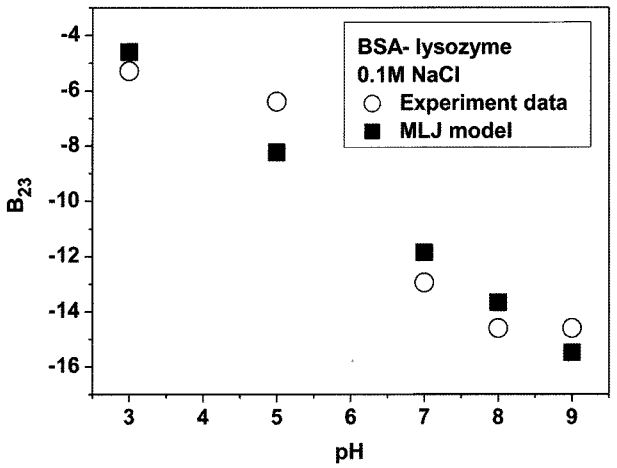

Figure 10. The cross 2nd virial coefficient as a function of pH with 0.1 M sodium chloride for BSA-lysozyme interaction. Circle symbols are experimental data and squares are calculated by eq. (2) with the MLJ potential.

tions become increasingly attractive. Above higher pH, the strength of attraction is expected to decrease slightly. At a given ionic strength, the strength of attraction due to electrostatic interactions is expected to be proportional to the product of the charges on the two proteins.

Conclusions

A new thermodynamic model is developed by introducing the MLJ pair potential function to calculate the osmotic cross second virial coefficient properties of two-protein systems under different solution conditions. The pair potential-energy function is proposed to explain the interaction between unfavorable proteins.

A temperature-dependent parameter, $A(\tilde{T})$, is determined from the computer simulation data for the compressibility factor. The minimum potential energy ε is then calculated from the experimental data and directly used to predict the osmotic cross second virial coefficient of BSA-lysozyme with various solution conditions with no additional model parameters. The proposed model shows good agreement with the experimental data of the given systems.

Acknowledgement. This work was supported by Seoul R&BD Program (CR070027). In Addition, the authors are grateful to Prof. J. M. Prausnitz from UC Berkeley for his valuable comments and help.

References

(1) Y. U. Moon, C. O. Anderson, H. W. Blanch, and J. M. Prausnitz, *Fluid Phase Equilib.*, **168**, 229 (2000).
(2) W. G. McMillan and J. E. Mayer, *J. Chem. Phys.*, **13**, 276 (1945).
(3) E. J W. Verwey and J. Th. G. Overbeek, *Theory of the Stabil-*

ity of Lyophobic Colloids, Elsevier, Amsterdam, 1948.
(4) C. A. Haynes, K. Tamura, H. R. Körfer, H. W. Blanch, and J. M. Prausnitz, *J. Phys. Chem.*, **96**, 905 (1992).
(5) V. L. Vilker, C. K. Colton, and K. A. Smith, *J. Colloid Interface Sci.*, **79**, 548 (1981).
(6) G. D. Phillies, *J. Chem. Phys.*, **60**, 2721 (1974).
(7) R. A. Curtis, J. M. Prausnitz, and H. W. Blanch, *Biotechnol. Bioeng.*, **57**, 11 (1998).
(8) P. M. Tessier, A. M. Lenhoff, and S. I. Sandler, *Biophis. J.*, **82**, 1620 (2002).
(9) S.Y. Patro and T. M. Przybycien, *Biotechnol. Bioeng.*, **52**, 193 (1996).
(10) P. M. Tessier, A. M. Lenhoff, and S. I. Sandler, *Biophys. J.*, **82**, 1620 (2002).
(11) P. M. Tessier, S. D. Vandrey, B. W. Berger, R. Pazhianur, S. I. Sandler, and A. M. Lenhoff, *Acta Crystallogr. Sect. D: Biol. Crystallogr.*, **58**, 1531 (2002).
(12) P. M. Tessier, H. R. Johnson, R. Pazhianur, B. W. Berger, J. L. Prentice, B. J. Bahnson, S. I. Sandler, and A. M. Lenhoff, *Proteins: Struct., Funct; Genet.*, **50**, 303 (2003).
(13) J. A. Barker and D. Henderson, *J. Chem. Phys.*, **47**, 4714 (1967).
(14) J. D. Weeks, D. Chandler, and H. C. Andersen, *J. Chem. Phys.*, **54**, 5237 (1971).
(15) J. Chang and S. I. Sandler, *Mol. Phys.*, **81**, 745 (1994).
(16) C. A. Teske, H. W. Blanch, and J. M. Prausnitz, *J. Phys. Chem. B*, **108**, 7437 (2004).
(17) P. L. Domen, J. R. Nevens, A. K. Mallia, G. T. Hermanson, and D. C. Klenk, *J. Chromatogr.*, **510**, 293 (1990).
(18) S. M. Walas, *Phase Equilibria in Chemical Engineering*, Butterworths, Boston, MA, 1985.
(19) S. Shen and B. C.-Y. Lu, *Fluid Phase Equilib.*, **84**, 9 (1993).
(20) J. Largo and J. R. Solana, *Phys. A*, **284**, 68 (2000).
(21) J. J. Nicolas, K. E. Gubbins, W. B. Streett, and D. J. Tidesley, *Mol. Phys.*, **37**, 1429 (1979).
(22) D. E. Kuehner, J. M. Prausnitz, F. Fergg, M. Wernick, H. W. Blanch, and J. Engmann, *J. Phys. Chem. B*, **103**, 1368 (1999).
(23) S. G. Kim and Y. C. Bae, *Macromol. Res.*, **10**, 67 (2003).
(24) N.Y. Jee and J. J. Kim, *Macromol. Res.*, **14**, 654 (2006).